IOPscience iopscience.iop.org

Home Search Collections Journals About Contact us My IOPscience

Post-implantation annealing of SiC studied by slow-positron spectroscopies

This article has been downloaded from IOPscience. Please scroll down to see the full text article.

1998 J. Phys.: Condens. Matter 10 1147

(http://iopscience.iop.org/0953-8984/10/5/022)

View the table of contents for this issue, or go to the journal homepage for more

Download details:
IP Address: 171.66.16.209
The article was downloaded on 14/05/2010 at 12:11

Please note that terms and conditions apply.

J. Phys.: Condens. Matter **10** (1998) 1147–1156. Printed in the UK PII: S0953-8984(98)87202-0

Post-implantation annealing of SiC studied by slow-positron spectroscopies

G Brauer†, W Anwand†, P G Coleman‡, J Störmer§, F Plazaola‖, J M Campillo‖, Y Pacaud† and W Skorupa†

† Institut für Ionenstrahlphysik und Materialforschung, Forschungszentrum Rossendorf, Postfach 510119, 01314 Dresden, Germany

‡ School of Physics, University of East Anglia, Norwich NR4 7TJ, UK

§ Institut für Nukleare Festkörperphysik, Universität der Bundeswehr München, 85577 Neubiberg, Germany

‖ Elektrika eta Elektronika Saila, Euskal Herriko Unibertsitatea, 644 p.k., 48080 Bilbo, Spain

Received 27 August 1997, in final form 17 November 1997

Abstract. The effects of post-implantation annealing of damage in 6H-SiC caused by ion implantation at two different fluences have been studied by monoenergetic positron Doppler broadening and lifetime techniques. The measurements are supported by new calculations of positron lifetimes in vacancy clusters in SiC. At both fluences two defected layers are identified and characterized by depth and defect type as a function of annealing temperature. The results indicate that it is impossible to remove the radiation damage by annealing at temperatures up to 1500 °C.

1. Introduction

Positron annihilation spectroscopy (PAS) is now a well established tool for the study of electronic and defect properties of solids [1, 2]. Recent developments in slow-positron beam methods [3] allow the extension of traditional techniques to investigations of thin films, layered structures and surfaces [4]. PAS is mostly applied to, and best understood, in metallic materials, but has found also application in the study of vacancy-type defects in semiconductors and has revealed information on ion-type acceptors via positron trapping at shallow Rydberg states [5]. Although elemental and compound (III–V, II–VI) semiconductors have been investigated in most experimental studies to date, SiC has recently attracted increased interest [6–13].

Radiation damage caused by the implantation of 200 keV Ge^+ ions into 6H-SiC has been studied recently by monoenergetic positron Doppler broadening and lifetime techniques [14]. Specimens exposed to seven ion fluences ranging from 10^{12} to 10^{15} cm^{-2}, together with unirradiated samples, were studied. The depth of the damaged crystalline layer was found to range from about 300 to 600 nm and, for ion fluences above 3×10^{13} cm^{-2}, an amorphous layer was seen whose thickness increased to 133 nm at the highest fluence. Positron lifetime measurements, in combination with theoretical calculations, suggest that the main defect produced is the divacancy, but that Si monovacancies are also created. In the amorphous surface layer larger agglomerates consisting of at least four, but more probably six, vacancies were detected. Furthermore, trapping rates were evaluated as a function of incident positron energy by applying the positron trapping model to the data.

 © 1998 IOP Publishing Ltd

Values for defect concentrations in the damaged layers of about 50 ppm were deduced by invoking plausible assumptions. In addition, the problem of extracting defect profiles from the data was discussed.

The aim of the present work is to study the effects of post-implantation thermal annealing of the radiation damage in 6H-SiC caused by implantation of 200 keV Ge^+ ions at two fluences (10^{14} and 10^{15} cm^{-2}). The techniques used are monoenergetic positron Doppler broadening and lifetime spectroscopies coupled with theoretical analysis.

The paper is organized as follows. In section 2 experimental details of the work are described. Section 3 contains the results of extended theoretical calculations of the positron lifetime in some SiC polytypes together with a presentation and discussion of the variable-energy positron measurements. Conclusions are presented in section 4.

2. Experimental details

Two single-crystalline, 25 mm diameter n-type 6H-SiC(0001) wafers (Si surface) were used as substrate materials [15]. The implantation was performed by 200 keV Ge^+ ions at room temperature to a fluence of 10^{14} cm^{-2} (wafer 1) and 10^{15} cm^{-2} (wafer 2). (Ge^+ ions have the same valency as Si and C and therefore lead to damage but no doping effects.) In order to minimize any possible uncertainty about the initial states of different specimens each wafer was implanted before being cut into four equally sized pieces. One piece served as the as-implanted reference sample and the three remaining pieces from each wafer were separately heat treated at predetermined temperatures of 500, 950 and 1500 °C. Treatment at the two lower temperatures was performed after encapsulation by a glass ampoule containing an Ar atmosphere. For heat treatment at 1500 °C the specimens were put into a closed graphite container evacuated to 10^{-4} Torr and filled with Ar at 760 Torr. The time of heat treatment at each temperature was 600 s.

For easier identification the specimens are labelled according to the code EUij. i is the wafer number (1 or 2) and j relates to the heat treatment (0 = as-implanted, 1 = 500 °C, 2 = 950 °C, 3 = 1500 °C). Use of this code is also helpful in comparison with the earlier results of [14].

A comprehensive review of positron beam techniques and their application is presented in [3]. In the present work variable-energy positron Doppler broadening measurements were performed at room temperature for all specimens using a computer-controlled magnetic-transport beam system at UEA Norwich [16]. Positron energies E between 0.1 and 30 keV were used. Energy spectra of annihilation gamma rays were measured with a Ge detector having an energy resolution (FWHM) of about 1.2 keV at 511 keV. The Doppler broadening of the annihilation line is caused by the momentum of the annihilating electron–positron pair and can be characterized by the lineshape parameter S. The value of S is defined as the integral of gamma ray intensity in the central energy region divided by the total intensity of the line. Sample characteristics such as damaged layer thicknesses and defect profiles are usually extracted from the $S(E)$ data by fitting with a program package such as VEPFIT [17].

Variable-energy positron lifetime measurements were performed with the timed beam system at UBW Munich [18] at room temperature. The mean lifetime $\tau(E)$ provides useful additional information about the type of defect involved. The lifetime spectra contained at least 10^6 events and were analysed using a modified version of the program package POSITRONFIT [19] using a stable, measured resolution function of 250 ps FWHM.

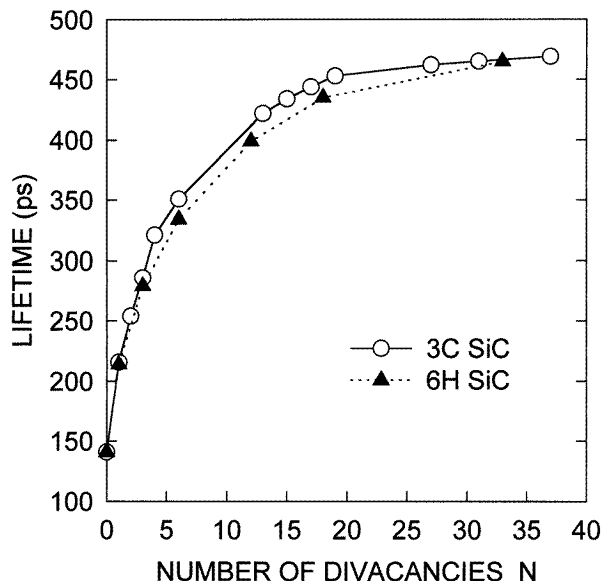

Figure 1. Calculated positron lifetime in vacancy clusters in 3C-SiC and 6H-SiC as a function of the cluster size N (N = number of Si–C divacancies).

3. Results and discussion

3.1. Theoretical calculations of positron lifetimes

Calculations using the superimposed atom model [20] have been performed for 3C-SiC and 6H-SiC polytypes in order to evaluate the positron lifetimes to be expected in larger clusters, containing several divacancies, which are thought to form after post-implantation annealing. Details of earlier calculations for the perfect lattice, as well as for several defected lattices containing smaller-sized defects, were published in [14]; the difference between those calculations and those presented here lies in the size of the supercells used. In the case of 3C-SiC the supercell is a cube containing 512 atoms in the perfect lattice, and $(520 - 2N)$ atoms for a cluster containing N divacancies. To simulate the 6H-SiC structure an orthorhombic supercell containing 720 atoms is used, and $(720 - 2N)$ atoms for the cluster with N divacancies.

The geometries of the vacancy clusters are chosen by building three-dimensional volumes as symmetrical as possible. However, in the case of the 6H-SiC structure this is not an easy task due to the complexity of the structure. The close-packing arrangement of this structure forms 'ABCACB' sequences for each type of atom, where the planes A, B and C are perpendicular to the c-axis. Both types of atom are separated along the c-axis by 0.189 nm (3.562 au) leading to the sequence unit $A_C A_{Si} B_C B_{Si} C_C C_{Si} A_C A_{Si} C_C C_{Si} B_C B_{Si}$. As divacancies have been taken away to build the unrelaxed clusters, the position of the divacancy is denoted by the position of the removed C atom (the corresponding Si atom taken away is located 0.189 nm above along the c-axis).

In the case of the 3C-SiC polytype C and Si atoms are separated along the diagonal of the cubic structure (i.e., the (111) axis) and a quite symmetric cluster used in the calculations is the one formed by 19 divacancies that corresponds to two octahedrons, one for each type of atom position, separated by $(3/4)^{1/2}$ lattice parameters along the (111) direction.

Figure 1 shows the trends of the calculated positron lifetimes as a function of the number of divacancies taken away to form the vacancy cluster in the two polytypes studied. Even though the trends are similar in both polytypes the lifetimes calculated in the 3C-SiC one are a little larger, indicating the difference in the free volume of the vacancy clusters caused by the different lattices. The positron lifetime increases rapidly when the cluster starts to grow and saturates at about 500 ps, which corresponds to the low-density limit of the interpolation formula of Brandt and Reinheimer [21]. The positron lifetime saturates at about the same size of clusters in both polytypes, i.e. about 20 divacancies, corresponding to a spherical volume radius of around 0.8 nm.

It should be noted that in the present calculations the relaxation of the atoms surrounding the vacancy cluster has not been taken into account. The inclusion of atomic relaxation in semiconductors is a very difficult task that to the authors' knowledge has only been performed in the case of single vacancies (e.g. in Si [22] and GaAs [23, 24]). Furthermore, relaxation may depend strongly on the charge state of the vacancy, and in these cases the trapping of a positron opposes inward relaxation [25]; it has been shown that if atomic relaxation is omitted then the charge state does not strongly affect the positron lifetime [26].

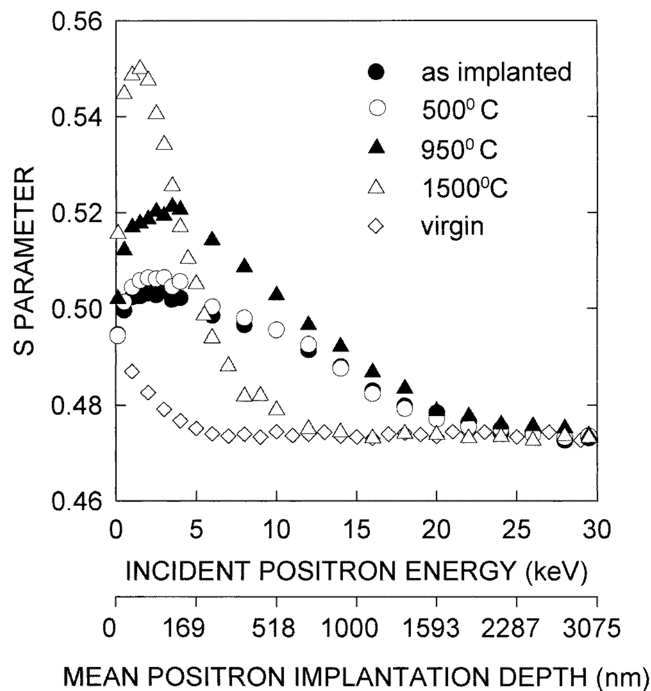

Figure 2. Mean Doppler broadening parameter S as a function of incident positron energy E for specimens EU10–EU13.

3.2. Damage at a fluence of 10^{14} cm^{-2} and changes after post-implantation annealing

$S(E)$ results for the as-implanted (EU10) and annealed (EU11, EU12, EU13) samples are presented in figure 2. The thicknesses d_i $(i = 1, 2)$ of two damaged layers [14] have been evaluated using the program VEPFIT [17]. The fit curves are not shown in figure 2, or in

later figures; they all pass smoothly through the data points. In addition, the ratio S_i/S_b for a given layer has been evaluated, where S_i is associated with the ith layer and S_b the virgin bulk. The diffusion length derived from the virgin SiC data (65 ± 3 nm), also shown in figure 2, has been used as a fixed value in all the evaluations presented in this paper. All the results are summarized in table 1. The uncertainties quoted are those given by VEPFIT, and are thus statistical; the possibility of significant systematic error arising from the non-uniqueness of the fitting procedure is minimal because the fitted parameters for all four samples in the series are physically meaningful and self-consistent.

Table 1. Characteristic parameters of damaged layers in specimens EU10–EU13 (fluence = 10^{14} cm^{-2}). d_i = thickness of layer i, S_i/S_b = Doppler broadening parameter ratio of layer i ($i = 1, 2$).

Sample	S_{d1}/S_b	d_1 (nm)	S_{d2}/S_b	d_2 (nm)
EU10	1.068	171 ± 26	1.054	662 ± 48
EU11	1.074	163 ± 18	1.056	598 ± 38
EU12	1.105	156 ± 12	1.078	476 ± 25
EU13	1.156	61 ± 1	—	—

It is evident that the layer thicknesses decrease after annealing at 500 °C, and that this trend continues at 950 °C. After annealing at 1500 °C only one narrow layer remains. The ratio S_i/S_b also undergoes considerable changes due to annealing. In the case of Si and GaAs it is known that the ratio S_d/S_b (d = defect) is 1.02–1.03 for a monovacancy, 1.03–1.04 for a divacancy and >1.05 for a larger vacancy cluster or void [5]. From our previous studies [14] it is known that the main defect in layer 2 is the divacancy, but that Si monovacancies are still present; this combination of defects in 6H-SiC is characterized by the ratio 1.05–1.06. As the divacancy concentration is much larger than the monovacancy concentration [14] it seems that the ratio S_d/S_b for divacancies in 6H-SiC is larger than that observed in Si and GaAs [5].

Positron lifetime measurements, combined with theoretical estimates (figure 1), give the approximate size of agglomerates in the samples. The mean lifetime results $\tau(E)$ seen in figure 3 show trends similar to those seen in $S(E)$ in figure 2, as expected. A two-component fit was possible for all spectra in the low-energy range. The aim of the following analysis is to identify defect lifetimes and not defected layer thicknesses.

In order to reduce the scattering of the data in the unconstrained fit, one component was fixed. A new software program allowed the quick analysis and comparison of all spectra measured for one sample at different energies, with the defect lifetime fixed values ranging from (for example) 200 to 350 ps in steps of 5 ps. Starting with the unconstrained fit, the value of the fixed defect lifetime was chosen using the criteria that (a) the variance of the fit should be close to a minimum, and (b) fixing of the shorter measured defect lifetime to a value in the range 200–250 ps should result either in a second, longer defect lifetime (>250 ps) or in a diffusion and trapping-reduced bulk lifetime (<155 ps). The choice of the fixed value was not always achieved unambiguously. As an example, in figure 4 the second (unconstrained) lifetime τ_2 found with the first lifetime fixed at $\tau_1 = 220$ ps is shown for specimen EU10. In the energy range 1–10 keV a longer defect lifetime is measured. The high points at around 10 keV are an artefact of the analysis associated with the vanishing of the long (τ_2) component. Above 10 keV the intensity of the long component is so small that only the (shorter) lifetime characteristic of the defect-free substrate is resolved.

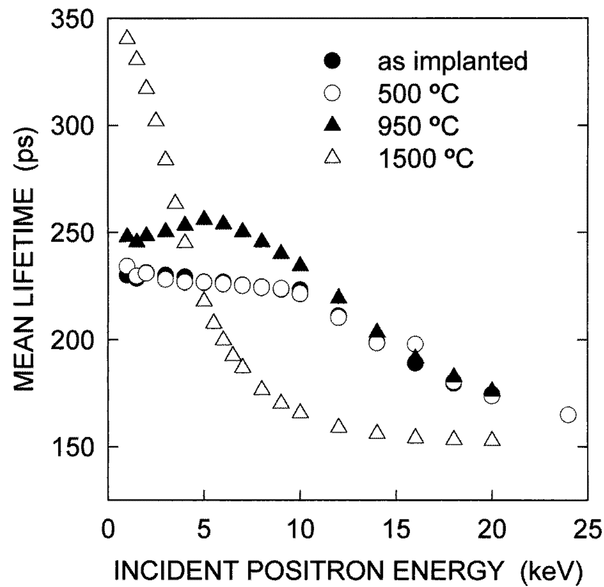

Figure 3. Mean positron lifetime τ as a function of incident positron energy E for specimens EU10–EU13.

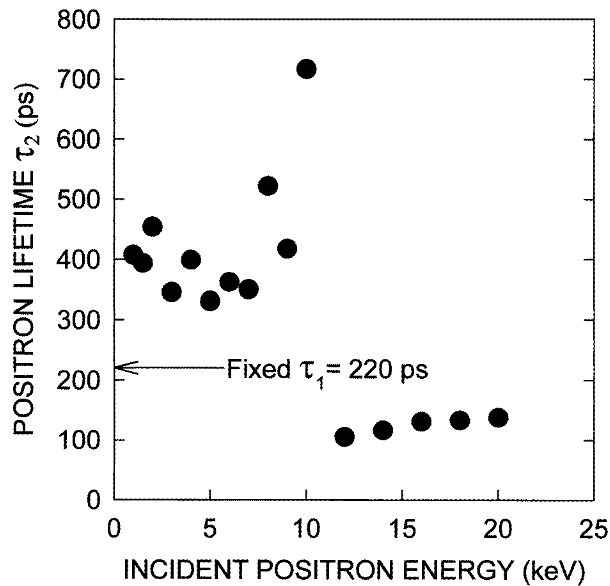

Figure 4. Unconstrained positron lifetime τ_2 as a function of incident positron energy E for specimen EU10, obtained by fixing the first lifetime τ_1 at 220 ps.

In table 2 the complete lifetime results for samples EU10–13 are collected. The values of the unconstrained lifetimes represent an averaged value, whereas I_{max} is the highest measured intensity value of the corresponding positron lifetime.

Table 2. Results of the lifetime analysis for specimens EU10–EU13 (fluence = 10^{14} cm^{-2}). The values of the unconstrained lifetimes represent an averaged value. I_{max} is the highest measured intensity value of the corresponding lifetime.

	EU10	EU11	EU12	EU13
τ_1 (ps)	220 ± 10 (fixed)	220 ± 10 (fixed)	205 ± 20	180 ± 20
τ_2 (ps)	398 ± 30	454 ± 30	318 ± 20 (fixed)	318 ± 20 (fixed)
Remarks	τ_2 for $E < 12$ keV with $I_{max} = 8\%$	τ_2 for $E < 12$ keV with $I_{max} = 6\%$	τ_2 with $I_{max} = 45\%$	τ_2 with $I_{max} = 71\%$

The present measurements indicate that the ratio τ_d/τ_b for 6H-SiC is $220/141 = 1.56$. While this is rather lower than the earlier experimental value of 1.68 [14], it is still significantly larger than the ratio of 1.3–1.4 for a divacancy in Si and GaAs [5].

3.3. Damage at a fluence of 10^{15} cm^{-2} and changes after post-implantation annealing

$S(E)$ results for the as-implanted (EU20) and annealed (EU21, EU22, EU23) samples are presented in figure 5. The thicknesses d_i ($i = 1, 2$) of the two damaged layers and the ratios S_i/S_b are summarized in table 3.

Table 3. Characteristic parameters of damaged layers in specimens EU20–EU23 (fluence = 10^{15} cm^{-2}). d_i = thickness of layer i, S_i/S_b = Doppler broadening parameter ratio of layer i ($i = 1, 2$).

Sample	S_{d1}/S_b	d_1 (nm)	S_{d2}/S_b	d_2 (nm)
EU20	1.097	192 ± 7	1.062	541 ± 24
EU21	1.108	163 ± 4	1.056	509 ± 21
EU22	1.141	94 ± 3	1.096	365 ± 11
EU23	1.126	14 ± 1	1.098	153 ± 4

As in the case of the lower fluence, the layer thicknesses start to decrease after annealing at 500 °C. This trend continues due to application of higher annealing temperatures but two layers always remain clearly distinguished.

The ratio S_i/S_b again changes significantly after annealing. It is obvious that in layer 2 positrons are mainly trapped in divacancies, as indicated by a ratio of about 1.06. Again, ratios larger than this value point to positron trapping in vacancy agglomerates or voids. The observation of decreasing layer thickness and agglomeration of vacancies after annealing is broadly consistent with the results of Uedono *et al* [13].

The mean lifetime results $\tau(E)$ seen in figure 6 mirror the $S(E)$ results in figure 5, as for the lower fluence. Results of the lifetime analysis are summarized in table 4. For EU22 an unexpected third long-lifetime component for $E < 5$ keV, fixed to 1.5 ns in the analysis, needs to be taken into consideration in order to perform a reasonable fit, with the second lifetime being fixed at 395 ps. The intensity of the very long lifetime varied in the range 0–4%.

3.4. Comments on the results for defect size

Except for the samples EU13 and EU23, all the samples show saturation trapping for implantation energies below 12 keV with two different defect types. In the case of EU22

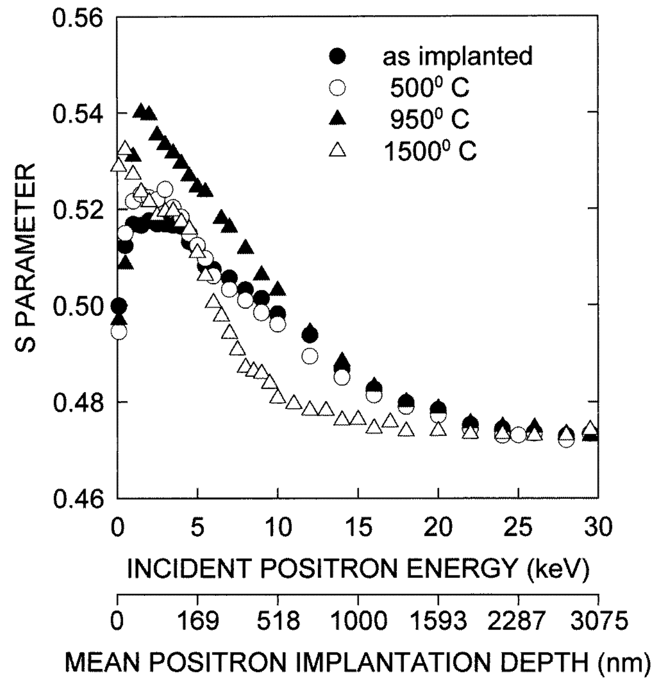

Figure 5. Mean Doppler broadening parameter S as a function of incident positron energy E for specimens EU20–EU23.

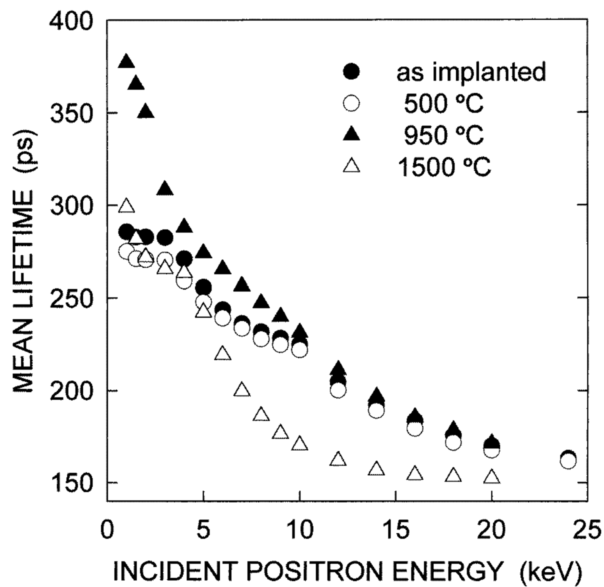

Figure 6. Mean positron lifetime τ as a function of incident positron energy E for specimens EU20–EU23.

the very long lifetime of 1.5 ns should be regarded an artefact due to the inability to describe the measured spectra fully with two components chosen. This gives an indication of the

Table 4. Results of the lifetime analysis for specimens EU20–EU23 (fluence = 10^{15} cm^{-2}). The values of the unconstrained lifetimes represent an averaged value. I_{max} is the highest measured intensity value of the corresponding lifetime.

	EU20	EU21	EU22	EU23
τ_1 (ps)	220 ± 10 (fixed)	215 ± 10 (fixed)	210 ± 20	180 ± 20
τ_2 (ps)	341 ± 30	320 ± 30	395 ± 20 (fixed)	425 ± 20 (fixed)
Remarks	τ_2 for $E < 12$ keV with $I_{max} = 72\%$	τ_2 for $E < 12$ keV with $I_{max} = 59\%$	τ_2 with $I_{max} = 89\%$ at $E = 10$ keV	τ_2 with $I_{max} = 43\%$

difficulties in describing the radiation damage in terms of a simple picture. The maximum intensities given therefore only allow estimation of the ratios of the total trapping rates.

The samples (except EU13 and EU23) show a defect characterized by a positron lifetime $\tau_d = 220$ (+10, −20) ps, which is in reasonable accordance with previously published results [14], where an experimental lifetime of $\tau_d = 235 \pm 3$ ps was attributed to the divacancy; indeed, the present measurement is even closer to the theoretically predicted lifetime of 214 ps for the divacancy [14, 27]. The corresponding S values lie in the range 1.054–1.062 (for EU10, EU11, EU20, EU21).

It needs to be noted that there seem to be some inconsistencies when comparing the $S(E)$ with the $\tau(E)$ results. For example, the lower normalized S values for EU12 and EU22 (1.078 and 1.096, respectively) do not correspond to the short defect lifetimes of 205 ps (EU12) and 210 ps (EU22), respectively. The reason for this is not quite clear and the present study therefore can only be regarded a first attempt to combine the results of both methods. Although the VEPFIT analysis of the $S(E)$ results takes into account diffusion processes, changes of the normalized S values of the order of 0.001 cannot easily be interpreted in the light of a change of the defect size. On the other hand, the lifetime analysis is no easy task either in such complicated structures as is indicated by the unexpected third lifetime component needed for a reasonable analysis of the data for EU22.

The longer defect lifetime of $\tau_d = 320$ ps (EU12 and EU21) corresponds to a normalized S value of 1.10 and represents an agglomeration of about seven divacancies (see figure 1). The defect lifetimes $\tau_d = 395$ ps (EU13, EU22) and 425 ps (EU23) correspond to normalized S values in the range between 1.126 (EU23) and 1.156 (EU13), and should therefore represent an agglomeration of about 13 and 16 divacancies, respectively.

4. Conclusions

The positron annihilation studies presented clearly demonstrate that it is not possible to anneal out the radiation damage caused by ion implantation at the fluences chosen even at 1500 °C.

Two layers showing different defect structures and thickness may be identified in SiC. After annealing at 500 and 950 °C the thickness of each layer is reduced and their defect structure changes, with the formation of vacancy agglomerates.

After annealing at 1500 °C only one narrow defected layer remains in the sample implanted at the lower fluence, having mainly agglomerates containing about 13 divacancies. After similar annealing the sample implanted at the higher fluence has two identifiable defected layers and defect agglomerates of 16 divacancies are found.

The ratios S_d/S_b and τ_d/τ_b for divacancies and voids seem to be larger in 6H-SiC compared to Si and GaAs [5].

Acknowledgment

This work was partly supported by EMRS-Network 3:IBOS (contract No ERBCHRX-CT93-0125).

References

[1] Brandt W and Dupasquier A (eds) 1983 *Positron Solid State Physics: Proc. Int. School Physics 'Enrico Fermi', Course 83 (Varenna, 1981)* (Amsterdam: North-Holland)
[2] Dupasquier A and Mills A P Jr (ed) 1995 *Positron Spectroscopy of Solids: Proc. Int. School Physics 'Enrico Fermi', Course 125 (Varenna, 1993)* (Amsterdam: IOS)
[3] Schultz P J and Lynn K G 1988 *Rev. Mod. Phys.* **60** 701
[4] Ishii A (ed) 1992 *Positrons at Metallic Surfaces* (Aedermannsdorf: Trans Tech)
[5] Hautojärvi P 1995 *Mater. Sci. Forum* **175–178** 47
[6] Forster M, Claudy W, Hermes H, Koch M, Maier K, Major J, Stoll H and Schaefer H-E 1992 *Mater. Sci. Forum* **105–110** 1005
[7] Puff W, Boumerzoug M, Brown J, Mascher P, Macdonald D, Simpson P J, Balogh A G, Hahn H, Chang W and Rose M 1995 *Appl. Phys.* A **61** 55
[8] Dannefaer S 1995 *Appl. Phys.* A **61** 59
[9] Itoh H, Yoshikawa M, Nashiyama I, Wei L, Tanigawa S, Misawa S, Okumura H and Yoshida S 1993 *Hyperfine Interact.* **79** 725
[10] Girka A I, Mokrushin A D, Mokhov E N, Svirida S V and Shishkin A V 1992 *Amorphous and Crystalline Silicon Carbide III* ed G L Harris, M G Spencer and C Y Yang (Berlin: Springer) pp 207–11
[11] Rempel A A, Schaefer H-E, Forster M and Girka A I 1994 *Covalent Ceramics II: Non-Oxides* ed A R Barron, G S Fishman, M A Fury and A F Hepp (Pittsburgh., PA: Materials Research Society) pp 299–304
[12] Rempel A A and Schaefer H-E 1995 *Appl. Phys.* A **61** 51
[13] Uedono A, Itoh H, Ohshima T, Aoki Y, Yoskikawa M, Nashiyama I, Okumura H, Yoshida S, Moriya T, Kawano T and Tanigawa S 1996 *Japan. J. Appl. Phys.* **35** 5986
[14] Brauer G, Anwand W, Pacaud Y, Skorupa W, Plazaola F, Coleman P G, Knights A P, Störmer J and Willutzki P 1996 *Phys. Rev.* B **54** 3084
[15] Cree Research, Durham, NC, USA
[16] Chilton N B and Coleman P G 1995 *Meas. Sci. Technol.* **6** 53
[17] van Veen A, Schut H, de Vries J, Hakvoort R A and Ijpma M R 1990 *Positron Beams for Solids and Surfaces* ed P J Schultz, G R Massoumi and P J Simpson (New York: American Institute of Physics) p 171
[18] Willutzki P, Störmer J, Kögel G, Sperr P, Britton D T, Steindl R and Triftshäuser W 1994 *Meas. Sci. Technol.* **5** 548
[19] Kirkegaard P and Eldrup M 1974 *Comput. Phys. Commun.* **7** 401
[20] Puska M J and Nieminen R M 1983 *J. Phys. F: Met. Phys.* **13** 333
[21] Brandt W and Reinheimer J 1971 *Phys. Lett.* **35A** 109
[22] Sugino O and Oshiyama A 1992 *Phys. Rev. Lett.* **68** 1858
[23] Laasonen K, Puska M J and Nieminen R M 1992 *Phys. Rev.* B **45** 4122
[24] Gilgien L, Galli G, Gygi F and Car R 1994 *Phys. Rev. Lett.* **72** 3214
[25] Puska M J, Seitsonen A P and Nieminen R M 1995 *Phys. Rev.* B **52** 1
[26] Alatalo M, Puska M J and Nieminen R M 1993 *J. Phys.: Condens. Matter* **5** L307
[27] Brauer G, Anwand W, Nicht E-M, Kuriplach J, Sob M, Wagner N, Coleman P G, Puska M J and Korhonen T 1996 *Phys. Rev.* B **54** 2512